Available online at www.sciencedirect.com
SCIENCE DIRECT®
International Journal of Heat and Mass Transfer 47 (2004) 5651–5663
International Journal of HEAT and MASS TRANSFER
www.elsevier.com/locate/ijhmt

Effects of rim location, rim height, and tip clearance on the tip and near tip region heat transfer of a gas turbine blade

Jae Su Kwak *, Jaeyong Ahn, Je-Chin Han

Turbine Heat Transfer Laboratory, Department of Mechanical Engineering, Texas A&M University, College Station, TX 77843-3123, USA

Received 22 December 2003; received in revised form 9 July 2004
Available online 16 September 2004

Abstract

Effects of the rim height and the tip gap clearance on the heat transfer coefficients on the blade tip and near tip regions were measured with two different rim geometries. The heat transfer coefficient distributions were measured using the transient single color capturing liquid crystals technique. Rims were located along (a) the pressure and the suction side (full-rim case) and (b) the suction side of the blade tip (suction side rim case). The rim heights were (a) 2.1%, (b) 4.2%, and (c) 6.3% and the blade tip gap clearances were (a) 1.0%, (b) 1.5%, and (c) 2.5% of the blade span. Tests were performed on a five-bladed linear cascade placed in a blowdown facility. The overall pressure ratio, inlet total pressure to exit static pressure, was 1.2, and the Reynolds number based on the exit velocity and the axial cord length was 1.1×10^6. The turbulence intensity level at the cascade inlet was 9.7%, and the inlet and exit Mach number were 0.25 and 0.59, respectively. It was found that higher rims reduce the heat transfer coefficients on the tip and shroud, but the reduction on the pressure and suction sides was not significant. The suction side rim case provided lower heat transfer coefficients on the blade tip and near tip regions than the full-rim case.

1. Introduction

In a gas turbine, a gap exists between the rotating blades and stationary shroud, called tip gap. Because of the pressure difference between the blade pressure and suction sides, hot gas flows through this tip gap, resulting in a thin boundary layer along with high heat transfer coefficients on the blade tip. To reduce the heat transfer level and thus reduce the thermal load on the blade tip region, many researches have been conducted. Mayle and Metzger [1], Metzger and Rued [2], Rued and Metzger [3] performed heat transfer studies using a simplified 2-D rectangular flat tip model. Metzger et al. [4] and Chyu et al. [5] investigated heat transfer in a simplified 2-D rectangular grooved tip model. They showed that the heat transfer in the upstream end of the cavity was greatly reduced compared to the flat tip. However, at the downstream of the cavity, the heat transfer levels for the grooved tip were higher due to flow reattachment inside the cavity. They also showed that the effect of the shroud velocity on the heat transfer coefficient was very small. Heyes et al. [6] studied tip leakage flow on plane and rimmed tips in a linear cascade and concluded that the use of a rimmed tip, especially a suction side rim tip,

* Corresponding author. Current address: Aeropropulsion Department, Korea Aerospace Research Institute, 45 Eoeun-Dong, Yuseong-Gu, Daejeon 305-333, Korea. Tel.: +1 979 845 3738; fax: +1 979 862 2418.
E-mail address: jchan@mengr.tamu.edu (J.S. Kwak).

0017-9310/$ - see front matter © 2004 Elsevier Ltd. All rights reserved.
doi:10.1016/j.ijheatmasstransfer.2004.07.029

Nomenclature

C	tip clearance gap (% of the blade span)
C_x	axial chord length of the blade (8.61 cm)
h	local convective heat transfer coefficient (W/m^2K)
H	height of the rim (% of the blade span)
k	thermal conductivity of blade tip material (0.18 W/m K)
P	exit static pressure
P_t	inlet total pressure
t	transition time for liquid crystals color change
TE	trailing edge of the blade
T_i	initial temperature of the test surface
T_m	temperature of the mainstream at the cascade inlet (recovery temperature)
T_w	color change temperature of the liquid crystals
X	axial distance (cm)

Greek symbols

α	thermal diffusivity of blade tip material ($1.25 \times 10^{-7} m^2/s$)
τ	step change of time

Subscripts

i	initial state
m	mainstream
t	total
w	wall
x	axial distance

was more beneficial than a flat tip in reducing the amount of the leakage flow. Metzger et al. [7] measured local heat flux using heat flux sensors in a rotating turbine rig with two different tip gaps. Kim et al. [8] and Kim and Metzger [9] studied heat transfer and film cooling effectiveness using a 2-D rectangular tip model. Yang and Diller [10] studied local heat transfer coefficients at a single location on a turbine blade tip model with a recessed cavity (rimmed tip) in a stationary linear cascade. Dunn and Haldeman [11] measured time averaged heat flux at a recessed blade tip for a full-scale rotating turbine stage at transonic vane exit conditions. Their results showed that the heat transfer coefficient (Nusselt number) at the mid and rear portion of the cavity floor was of the same order as the blade leading edge value. Bunker et al. [12] investigated the detailed heat transfer coefficient distribution on a power generation turbine blade tip surface using a hue detection based liquid crystal technique, which was the first study to provide complete surface information. They measured the heat transfer coefficient at three tip gaps and two free-stream turbulence levels with both sharp and rounded edges. Azad and coworkers [13,14] studied the heat transfer on the first stage blade tip of an aircraft engine turbine (GE-E^3). They presented the effects of tip gap clearance and free-stream turbulence intensity level on the detailed heat transfer coefficient distributions for both the plane and rimmed tips in a stationary linear cascade under engine representative flow conditions. Teng et al. [15] measured the heat transfer coefficients and static pressure distributions of a turbine blade tip region in a large-scale low-speed wind tunnel facility using a transient liquid crystal technique. Bunker and Bailey [16] studied the effect of rim height and oxidation on turbine blade tip heat transfer with a power generation turbine blade. They showed that the effect of rim height is not uniform over the entire tip surface, but generally, a higher rim produced lower heat transfer coefficients. Their results also showed that blade tip heat transfer had low sensitivity to clearance gap magnitude. Azad et al. [17] also studied the effect of rim geometry arrangement on gas turbine blade tip heat transfer and found that the location of the rim could change the leakage flow and result in different heat loads on the blade tip. They also found that the suction side rim provided the lowest heat transfer coefficient among all the cases they studied. Rhee et al. [18] studied the local heat/mass transfer on the stationary shroud with blade tip clearances for flat tip geometry. They used the naphthalene sublimation method and concluded that the heat/mass transfer characteristics changed significantly with the gap clearance. Kwak and Han [19,20] presented heat transfer coefficients on the tip and near tip regions of both plane and rimmed tip blades. They showed that the rimmed tip could reduce heat transfer coefficients on the blade tip and the shroud. Papa et al. [21] measured average and local mass transfer coefficients on a rimmed tip and winglet-rimmed tip using naphthalene sublimation technique. They also presented flow visualization on the tip surface using an oil dot technique. Jin and Goldstein [22,23] measured local mass transfer on a simulated high pressure turbine blade and near tip surfaces. They showed that the averaged mass transfer rate on the tip surface was much higher than that on the suction and the pressure surface. Kwak et al. [24] studied the effect of the rimmed geometry and the tip gap clearance on the heat transfer coefficients on tip and near tip regions. They showed that the heat transfer coefficients on the blade tip and the shroud were significantly reduced by using a rimmed tip blade. However, the reduction in the heat transfer coefficients on the blade pressure and suction side was not remarkable. Their re-

sults also showed that the location of the high heat transfer region varied by changing the arrangement of the rims and the overall heat transfer coefficient on the tip for the suction side rim case was lower than other rimmed tip arrangement cases.

Numerical studies to investigate blade tip heat transfer have also been conducted. Ameri and Steinthorsson [25,26] predicted heat transfer on the tip of the Space Shuttle Main Engine (SSME) rotor blade. Ameri et al. [27] also predicted the effects of tip gap clearance and casing recess on heat transfer and stage efficiency for several rimmed blade tip geometries. Ameri and Bunker [28] performed a computational study to investigate the detailed heat transfer distributions on blade tip surfaces for a large power generation turbine and compared the result with the experimental data of Bunker et al. [12]. Ameri and Rigby [29] calculated heat transfer and film-cooling effectiveness on film cooled turbine blade models. Ameri [30] predicted heat transfer and flow on the blade tip of a gas turbine equipped with a mean-camber line strip. Ameri et al. [31] and Yang et al. [32,33] conducted numerical studies on the heat transfer on the rimmed tip blade.

A parametric study has been performed by investigating the effects of tip clearance and the rim height on the heat transfer coefficients on the tip surface, the shroud, and near the tip regions of the blade pressure and suction side. A previous study performed in this area by Bunker and Bailey [16] concentrated only on the effect of rim height for a power generation turbine blade and did not study the effect of tip gap clearance. They obtained heat transfer coefficient distributions only on the blade tip surface for one rim geometry (i.e. full rim case). In the present study, a comprehensive investigation has been performed not only to understand the effect of rim height and tip gap clearance but also to provide an optimum geometry for the blade tip for minimum heat transfer on the blade tip, shroud, near tip pressure side as well as near tip suction side for an aircraft turbine blade. The optimum geometry for the rim arrangement has been chosen based on the data provided by Kwak et al. [24], in which six different geometries of rim along the pressure and suction sides (full-rim case), suction side rim, pressure side rim, camber line rim, and their combinations were considered. They tested these six geometries for one rim height (H = 4.2%) with three different tip gap clearances of 1.0%, 1.5% and 2.5% of blade span and found that suction side rim case performed better in lowering blade tip heat transfer than the other cases. One of the primary objectives of this study is to determine whether this is still true at different rim heights.

A scaled up blade tip profile of a first stage rotor blade of a modern aircraft gas turbine (GE-E^3) was used in a 5-blade linear cascade with the center blade tip and near tip regions coated with liquid crystals. The same test section and flow loop were used by Kwak et al. [24] to study the best performing rim geometry. In the present study, heat transfer coefficient distributions have been obtained for the blade tip, shroud, and near tip region of pressure side and suction side for full side rim and suction side rim cases. Experiments were carried out at the three rim heights (H = 2.1%, 4.2%, and 6.3% of blade span) and the three tip gap clearances (C = 1.0%, 1.5%, and 2.5% of blade span). This research paper provides comprehensive information about the effects of rim heights on the blade tip heat transfer for the two best possible geometries of a rimmed tip blade.

2. Experimental setup

Fig. 1 shows the schematic of the blowdown test facility. Compressed air from a high pressure tank was made to flow through the loop via a pressure controller and a pneumatic control valve which maintained the flow to ±3% of mainstream flow with the help of feedback pressure from the downstream side. Steady flow

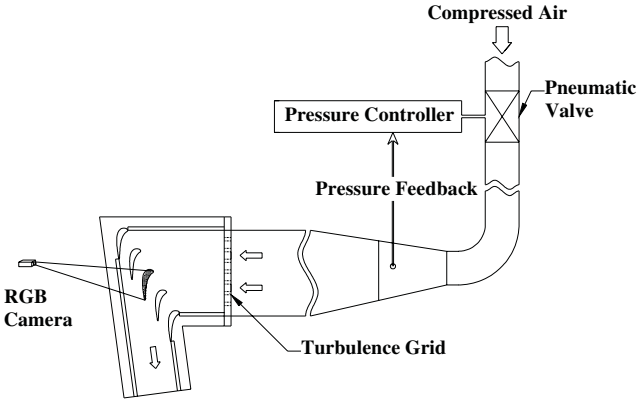

Fig. 1. Schematic of the blowdown facility.

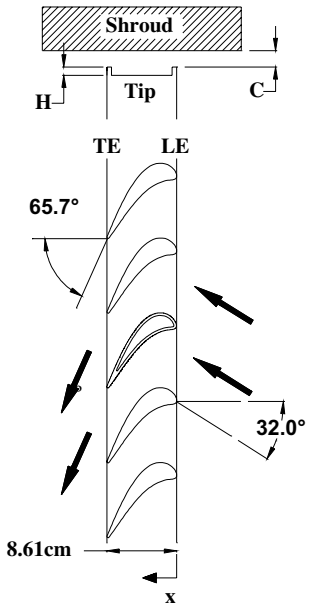

Fig. 2. Definition of blade tip and shroud.

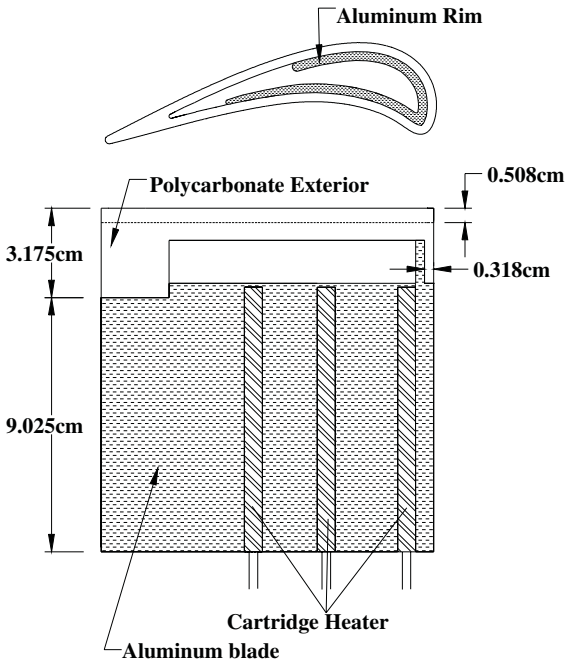

Fig. 3. Heat transfer measurement blade.

was obtained within 1.5 s of valve activation. During the blowdown test, the cascade inlet and exit air velocities were 85 m/s and 199 m/s, and the inlet and exit Mach numbers were 0.25 and 0.59, respectively. The turbulence intensity measured 6 cm upstream of the center blade was 9.7% and the turbulence length scale was estimated to be 1.5 cm. A turbulence grid with 57% porosity was placed before the entrance of the test section to achieve the above mentioned turbulence intensity. The Reynolds number based on axial chord length and exit velocity was 1.1×10^6. The inlet total pressure (P_t) was 126.9 kPa, and the exit static pressure (P) was 102.7 kPa, which gave an overall pressure ratio (P_t/P) of 1.2. Note that inlet total pressure was measured at the same measuring point of the turbulence intensity, which locates at the downstream of the turbulence grid. Azad et al. [13,14] has described the detailed flow conditions, including the flow periodicity in cascade. The rim heights used for this study were about 2.1%, 4.2%, and 6.3% and the tip gap clearance was 1.0%, 1.5%, and 2.5% of the blade span (12.2 cm). The definitions of blade tip and shroud are also shown in the upper part of Fig. 2. The blade had a 12.2 cm span and an 8.61 cm axial chord length. This was three times larger than the dimension of a GE-E^3 blade tip profile. Each blade had a constant cross-section for the entire span as shown in the lower part of Fig. 2. Fig. 3 shows the heat transfer measurement blade. The lower portion of the blade was made of aluminum with an inner rim. The upper tip portion was mounted on this rim by sliding it from the top. The upper tip portions were made of polycarbonate with low thermal conductivity. Cartridge heaters were inserted into the blade to heat the lower aluminum portion and, consequently, the upper tip portion. For the heat transfer measurement on the shroud, a 300 W plate heater was used to heat the shroud plate and was removed before the test. Fig. 4 shows detailed geom-

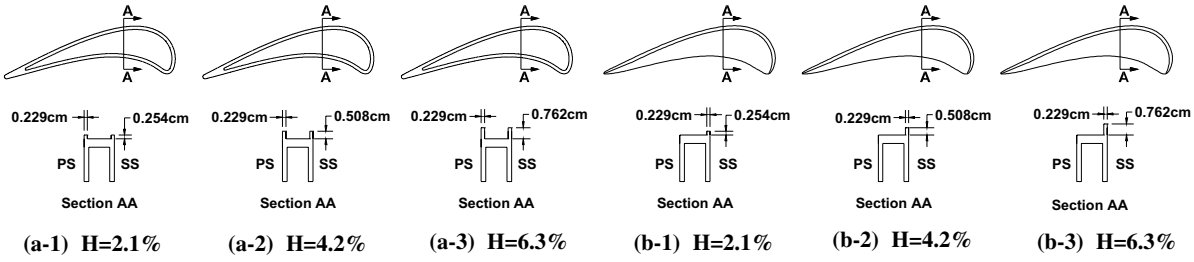

Fig. 4. Geometry of rimmed tips: (a) Full side rim; (b) suction side rim.

etries of the upper tip portions with full-rim (Fig. 4(a)) and suction side rim (Fig. 4(b)) for different rim heights.

3. Heat transfer measurement theory

A transient single color capturing liquid crystals technique was used to measure the heat transfer coefficient on the blade tip. The local heat transfer coefficient over a liquid crystal coated surface can be obtained using a one-dimensional semi-infinite solid assumption with convective boundary condition at the test surface. The solution for the 1-D transient conduction equation at the surface is:

$$\frac{T_w - T_i}{T_m - T_i} = 1 - \exp\left(\frac{h^2 \alpha t}{k^2}\right)\operatorname{erfc}\left(\frac{h\sqrt{\alpha t}}{k}\right) \quad (1)$$

By knowing the initial temperature (T_i) of the test surface, the mainstream (recovery) temperature (T_m) at the cascade inlet and the color change temperature (T_w) at time t, the local heat transfer coefficient (h) can be calculated from Eq. (1). If the mainstream temperature changes with time, the varying temperature can be represented as a series of step changes. Using Duhamel's superposition theorem, Eq. (1) can be written as follows:

$$T_w - T_i = \{T_{m,0} - T_i\} \times F\left(\frac{h\sqrt{\alpha t}}{k}\right) + \sum_{j=1}^{n}\left[F\left(\frac{h\sqrt{\alpha(t-\tau_j)}}{k}\right)\Delta T_{m,j}\right], \quad (2)$$

where

$$F(x) = 1 - \exp(x^2)\operatorname{erfc}(x),$$

where ΔT_m is the step changes in the mainstream.

The experimental uncertainty was calculated by the methods of Kline and McClintock [34]. It can be noted that the blade tip material (polycarbonate) has a very low thermal conductivity of 0.18 W/m K. The liquid crystals color change transition occurs at the surface, which is kept at a uniform initial temperature. Test duration is smaller (10–30 s) than the time required for the temperature to penetrate the full thickness of the blade tip material. Thus a 1-D transition, semi-infinite solid assumption is valid throughout the surface, except near the tip edges. The individual uncertainties in the measurement of the time of color change ($\Delta t = \pm 0.5$ s), the mainstream temperature ($\Delta T_m = \pm 0.5$ °C), the color change temperature ($\Delta T_w = \pm 0.2$ °C), the initial temperature ($\Delta T_i = \pm 1$ °C), and the blade tip material properties ($\Delta\alpha/k^2 = \pm 5\%$) were included in the calculation of the overall uncertainty of heat transfer coefficient. The uncertainty for the local heat transfer coefficient was estimated to be ±8% in most areas. However, the uncertainty in the high heat transfer region was estimated to be ±11% because the uncertainty in the color change time plays greater role if the color change time is short (approximately 5 s). In addition, the heat transfer coefficient near the blade tip edge might be overestimated as much as 15% due to the 2-D heat conduction effect.

4. Heat transfer measurement and results

Two different liquid crystals were used in this study. The 20 °C bandwidth liquid crystals (R34C20W, Hallcrest) were used to measure the initial temperature of the test surface, and the 4 °C bandwidth liquid crystals (R29C4W, Hallcrest) were used to measure the color changing time. Fig. 5(a) shows the results of the calibration for both the liquid crystals. Before the transient test, the initial temperature of the test surface was measured using the 20 °C bandwidth liquid crystals and Fig. 5(b) presents the initial temperature on the tip ($C = 1.5\%$, $H = 4.2\%$, suction side rim case). After the initial temperature measurement on the test surface, the color change of the liquid crystals was recorded at a speed of 30 frames per second using the 4 °C bandwidth liquid crystals. From every pixel at each stored image, the hue was evaluated and calculated the time from the initial condition to a pre-determined hue value. This time information was used in Eq. (2) to calculate the local heat transfer coefficient. The test duration time was short enough (10–30 s) to make a 1-D semi-infinite solid assumption. The detailed experimental procedure has been described by Kwak and Han [19,20].

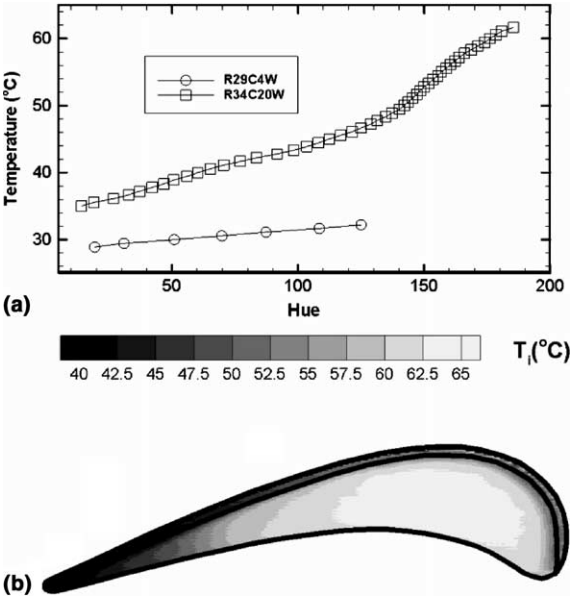

Fig. 5. (a) The relation between hue and temperature. (b) Initial temperature on the tip for the suction side rim with $H = 4.2\%$.

4.1. Heat transfer coefficient on the blade tip

Fig. 6 shows the heat transfer coefficient on the blade tip. Due to the shadow of the rim, data near the rim could not be taken. The plane tip cases (Fig. 6(g)) with three different tip gap clearances are presented for comparison. The detailed results of the plane tip case have been discussed by Kwak and Han [19].

The overall heat transfer coefficient for the rimmed tip cases shows lower heat transfer coefficient than the plane tip case. For the plane tip case (Fig. 6(g)), the maximum heat transfer coefficient can be seen near the pressure side and the value of the maximum heat transfer coefficient is about 1350 W/m^2K. On the other hand, the maximum value of the heat transfer coefficient on the tip for the rimmed tip cases is about 1000 W/m^2K and occurs on the rim.

Fig. 6(a) and (b) presents the heat transfer coefficients on the blade tip with two different tip geometries with three rim heights at $C = 1.5\%$. As the rim height increases from $H = 2.1\%$ to $H = 6.3\%$, the heat transfer coefficients on the tip decreases. Compared to the plane tip case with same tip gap clearance of 1.5% (Fig. 6(g-2)), the rimmed tip cases (Fig. 6(a) and (b)) show much low heat transfer coefficient. For the rimmed tip cases, the heat transfer coefficient on the rim is generally higher than on the tip surface and comparable to the high heat transfer coefficient of the plane tip case.

For the full side rim case (Fig. 6(a)), a high heat transfer coefficient region exists near the leading edge and this region is caused by the reattachment of the leakage flow as shown in Fig. 7(a)–(c). Fig. 7 shows the conceptual view of the flow near the tip region for the different tip geometries. In the full side rim cases, (Fig. 7(a)–(c)), the leakage flow reattaches to the tip surface near the suction side rim and a flow recirculation occurs in the cavity near the pressure side rim. The recirculation and the reattachment result in a lower heat transfer coefficient region near the pressure side rim and a higher heat transfer coefficient regions near the suction side rim, respectively. As the rim height increases from $H = 2.1\%$ (Fig. 7(a)), to $H = 6.3\%$ (Fig. 7(c)), the recirculation region becomes bigger and consequently, the heat transfer coefficient in the region becomes lower as shown in Fig. 6(a). In the suction side rim cases (Fig. 7(d)–(f)), the leakage flow reattaches to the tip surface near the pressure side and results in a high heat transfer coefficient in that region. Near the rim, a recirculation region exists and results in lower heat transfer coefficient. As the rim height increases from $H = 2.1\%$ (Fig.

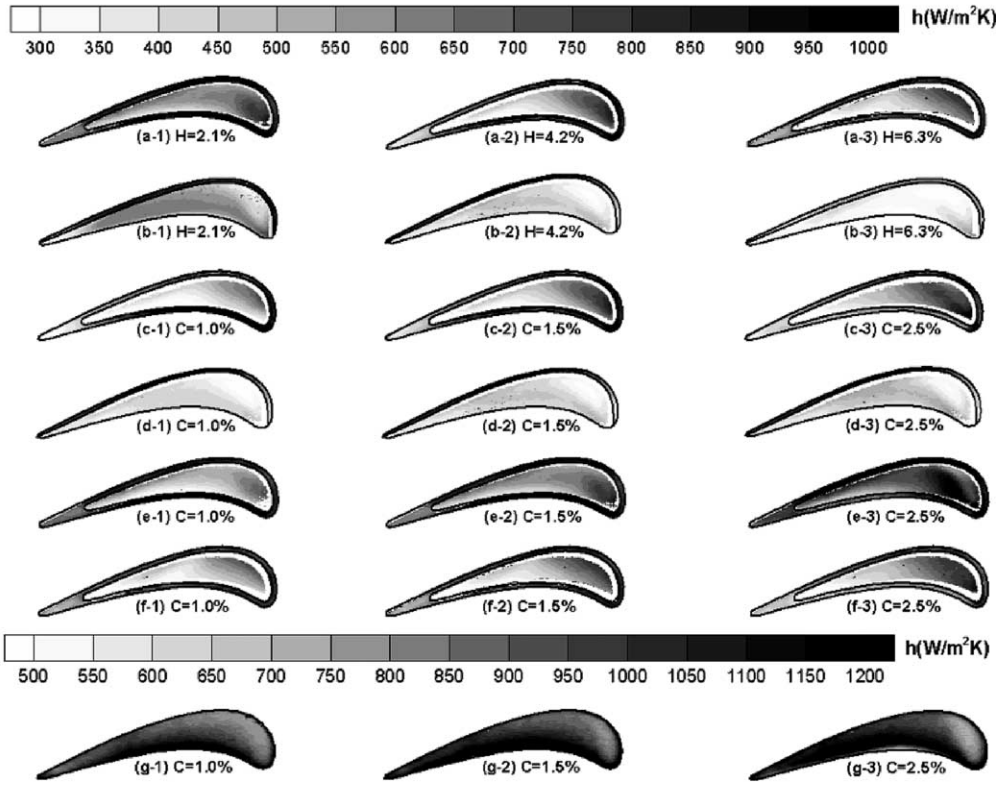

Fig. 6. Heat transfer coefficient on the tip. (a) Full side rim ($C = 1.5\%$); (b) suction side rim ($C = 1.5\%$); (c) full side rim ($H = 4.2\%$, [20]); (d) suction side rim ($H = 4.2\%$, [24]); (e) full side rim ($H = 2.1\%$); (f) full side rim ($H = 6.3\%$); (g) plane tip [19].

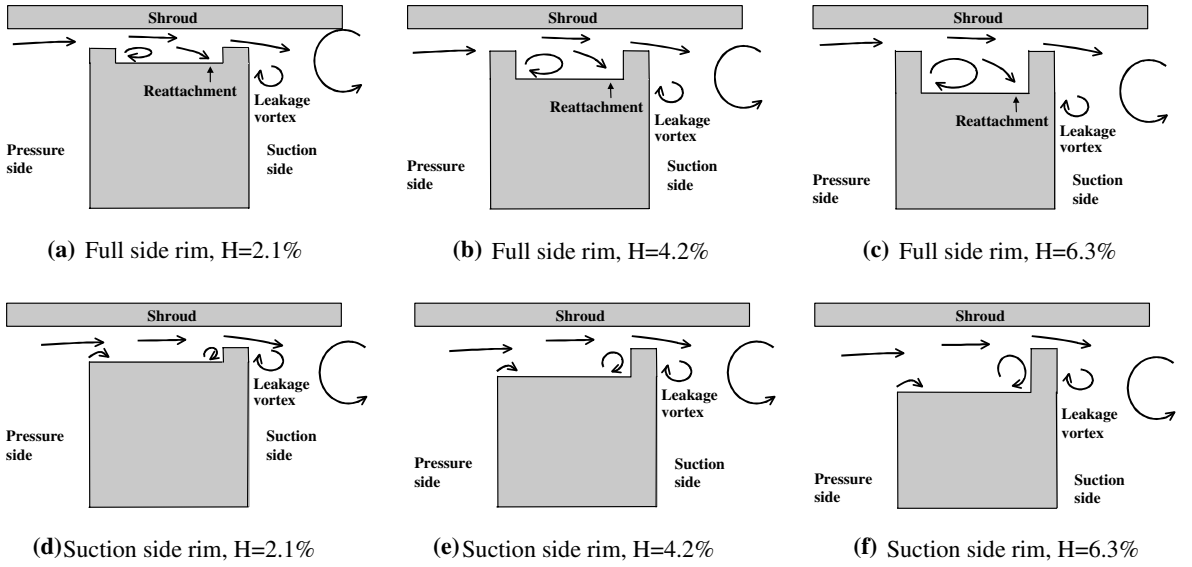

Fig. 7. The conceptual view of the flow near the tip region. (a) Full side rim, $H = 2.1\%$; (b) full side rim, $H = 4.2\%$; (c) full side rim, $H = 6.3\%$; (d) suction side rim, $H = 2.1\%$; (e) suction side rim, $H = 4.2\%$; (f) suction side rim, $H = 6.3\%$.

7(d)) to $H = 6.3\%$ (Fig. 7(f)), the heat transfer coefficient on the tip surface near the rim becomes lower (shown in Fig. 6(b)) as a result of the stronger recirculation region.

For the full side rim case (Fig. 6(a)), the overall heat transfer coefficient becomes lower as the rim height increases due to the increased flow resistance. Near the blade leading edge, the flow reattachment of the leakage flow is the dominant phenomenon and results in a high heat transfer coefficient region. Near the blade trailing edge, due to the relatively narrow cavity, the recirculation of the flow has a dominant effect on the heat transfer coefficient and results in lower heat transfer coefficient.

Fig. 6(b) presents the heat transfer coefficient distribution of suction side rim case. The overall heat transfer coefficient on the tip for this case is smaller than that for the full side rim case. There is a relatively low heat transfer coefficient region on the tip surface near the rim close to the leading edge. This region is caused by the recirculation of the flow near the rim as shown in Fig. 7(d)–(f). The heat transfer coefficient on this region decreases as the rim height increases. As the rim height increases, the overall heat transfer coefficient on the tip decreases.

Fig. 6(c), (e), and (f), which correspond to rim heights of $H = 4.2\%$, 2.1%, and 6.3% respectively, show the heat transfer coefficient on the tip with full side rim cases for the three rim heights with three tip gap clearances. As the tip gap clearance increases from $C = 1.0\%$ to $C = 2.5\%$, the heat transfer coefficient on the tip increases for a given rim height. At the same tip gap clearance, the heat transfer coefficient on the tip decreases as the rim height increases from $H = 2.1\%$ to $H = 6.3\%$. Fig. 6(d) presents the heat transfer coefficient on the tip for suction side rim case. This case also shows that the heat transfer coefficient on the tip increases as the tip gap clearance increases. Compared to full side rim cases (Fig. 6(c), (e), and (f)), suction side rim case (Fig. 6(d)) shows lower heat transfer coefficient at all tip gap clearances.

4.2. Heat transfer coefficient on the shroud surface

Fig. 8 shows the heat transfer coefficient on the shroud, opposite to the blade tip. The plane tip case (Fig. 8(g)) is presented for comparison. The detailed results for the plane tip are discussed by Kwak and Han [19]. Note that the experiments were conducted in a stationary cascade and its results cannot be applied to the actual rotating case directly.

For the rimmed tip cases (Fig. 8(a)–(f)), the high heat transfer coefficient region begins above the rim and extends to the downstream from the rim. The flow infiltrated between the rim and shroud impinges on the shroud and results in a high heat transfer coefficient at the downstream of the rim. Compared to the plane tip case (Fig. 8(g)), the rimmed tip cases show lower heat transfer coefficient. The maximum value of the heat transfer coefficient on the shroud is about $700\,W/m^2K$, which is about 70% of the maximum value of the tip surface.

Fig. 8(a) and (b) shows the heat transfer coefficient on the shroud for three different rim heights and two rim arrangements. Both cases show that the overall heat transfer coefficient on the shroud slightly decreases as

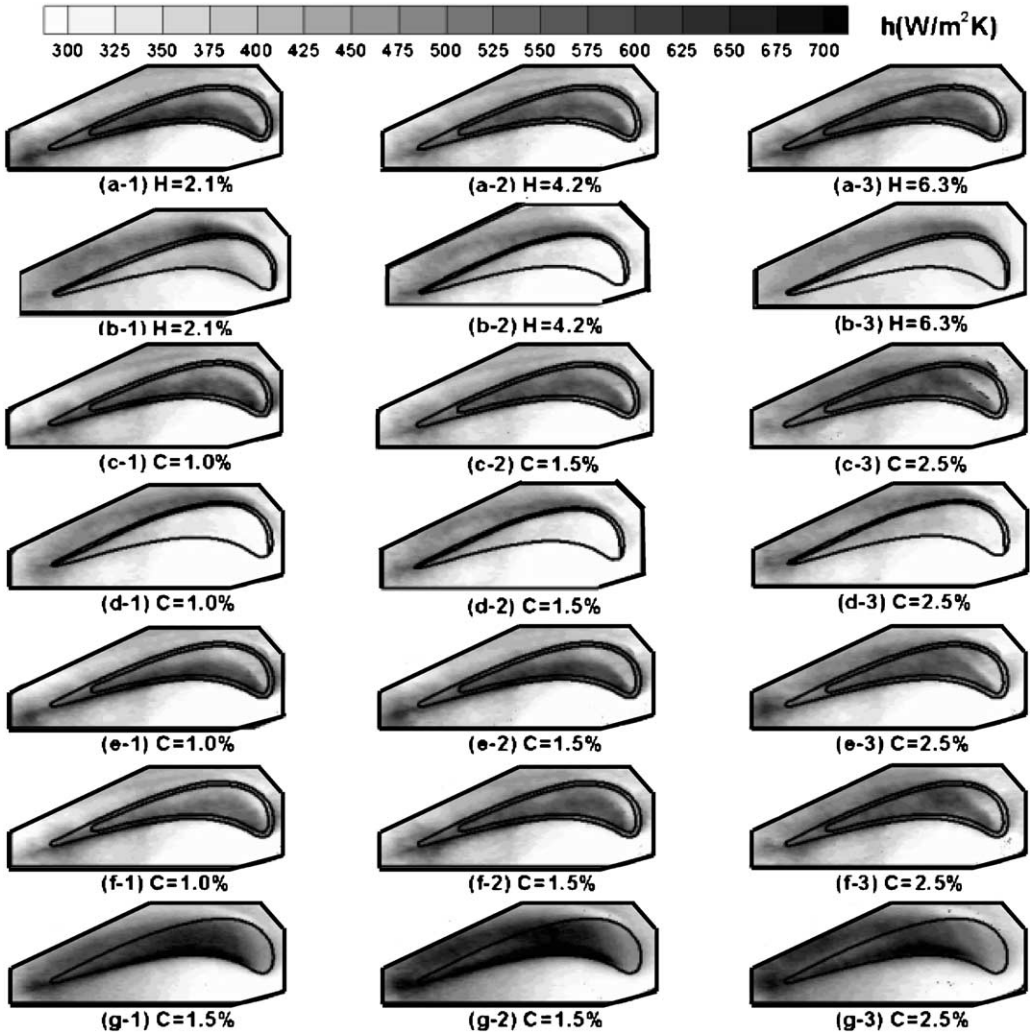

Fig. 8. Heat transfer coefficient on the shroud. (a) Full side rim (C = 1.5%); (b) suction side rim (C = 1.5%); (c) full side rim (H = 4.2%, [20]); (d) suction side rim (H = 4.2%, [24]); (e) full side rim (H = 2.1%); (f) full side rim (H = 6.3%); (g) plane tip [19].

the rim height increases. Compared to the full side rim case (Fig. 8(a)), the overall heat transfer coefficient on the shroud above the blade tip is lower for the suction side rim case (Fig. 8(b)).

Fig. 8(c), (e), and (f), which correspond to rim heights of H = 4.2%, 2.1%, and 6.3% respectively, show the heat transfer coefficient on the shroud for the full side rim cases for the three rim heights with three tip gap clearances. Generally, the overall heat transfer coefficient increases as the tip gap clearance increases from C = 1.0% to C = 2.5%. At the same tip gap clearance, higher rim case shows lower heat transfer coefficient.

For the suction side rim case with different tip gap clearances (Fig. 8(d)), the overall heat transfer coefficient on the shroud increases slightly as the tip gap clearance increases. The overall heat transfer coefficient for the suction side rim cases is lower than the full side cases.

4.3. Heat transfer coefficient on the near tip region of the pressure side

Fig. 9 shows the heat transfer coefficient distribution on the near tip region of the pressure side. The height of the measurement area was about 2.5 cm from the top of the rim (about 20% of the blade span). The plane tip case with different tip gap clearances is presented for comparison. The detailed results for the plane tip case are discussed by Kwak and Han [19].

All cases show that the heat transfer coefficient near the trailing edge is higher than near the mid chord region. This is caused by the boundary layer transition on the pressure side surface in streamwise direction. All the variations on rim geometries hardly affected the heat transfer coefficient on the near tip region of the pressure side.

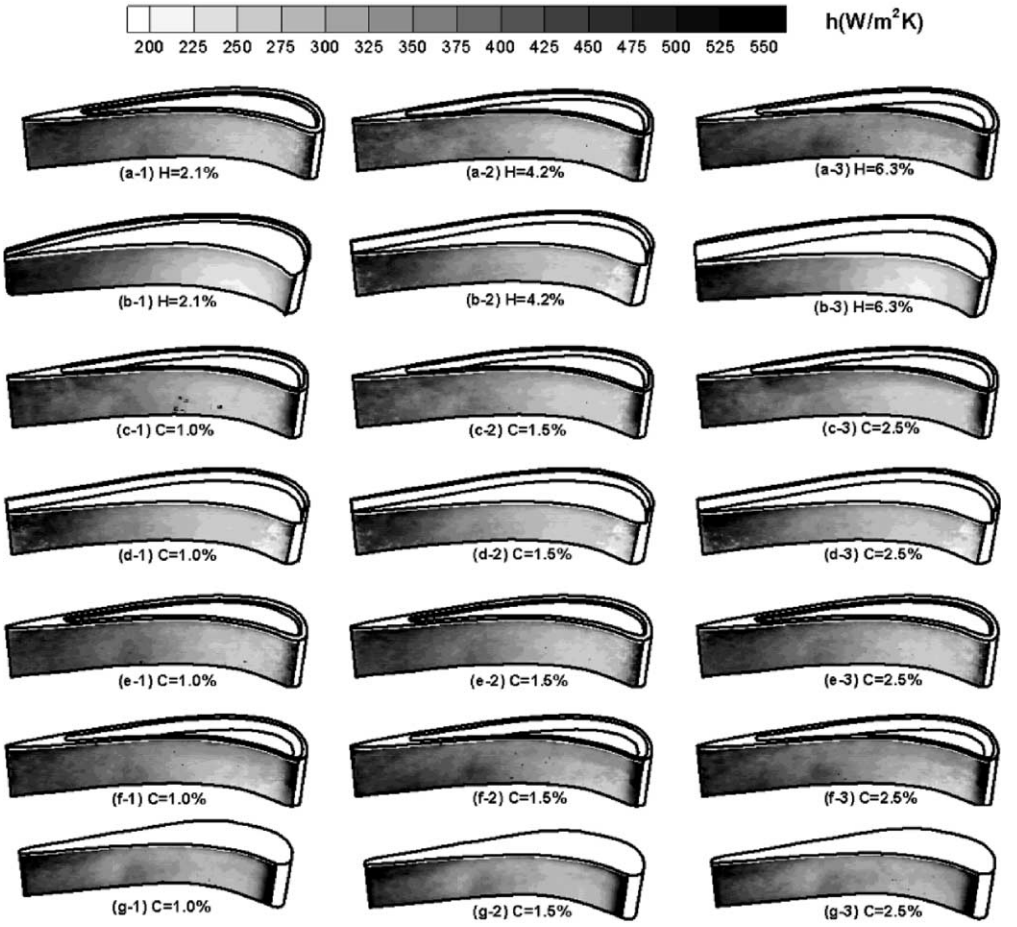

Fig. 9. Heat transfer coefficient on the near tip region of the pressure side. (a) Full side rim ($C = 1.5\%$); (b) suction side rim ($C = 1.5\%$); (c) full side rim ($H = 4.2\%$, [20]); (d) suction side rim ($H = 4.2\%$, [24]); (e) full side rim ($H = 2.1\%$); (f) full side rim ($H = 6.3\%$); (g) plane tip [19].

The maximum value of the heat transfer coefficient on the near tip of the pressure side is about 500 W/m^2K, which is about 50% of the maximum value on the tip surface. Generally, the overall heat transfer coefficient on the pressure side is lower than on the tip or the shroud surface.

4.4. Heat transfer coefficient on the near tip region of the suction side

Fig. 10 shows the heat transfer coefficient on the near tip region of the suction side. The height of the measurement area was about 20% of the blade span. The plane case with different tip gap clearances is presented for comparison. The detailed results of the plane tip case are discussed by Kwak and Han [19].

The overall heat transfer coefficient for the rimmed tip cases (Fig. 10(a)–(f)) is lower than that for the plane tip case (Fig. 10(g)). The maximum value of the heat transfer coefficient for the rimmed tip cases is about 70% of that on the plane tip case and is comparable with a maximum value of the shroud surface.

All cases show a high heat transfer coefficient region along the suction side tip. The high heat transfer coefficient in the region is caused by the leakage vortex. As the leakage flow exits from the tip gap to the suction side of the blade, the leakage flow separates from the tip or rim surface and forms a leakage vortex as a result of the interaction with the mainstream flow as shown in Fig. 7. For the full side rim cases (Fig. 10(a), (c), (e), and (f)) and the plane tip case (Fig. 10(g)), the trace of the leakage vortex is clearly seen along on the near tip region of the blade suction side. For the suction side rim cases (Fig. 10(b) and (d)), the size of the trace of the leakage vortex is much smaller than the other cases. The heat transfer coefficients on the tip and shroud for the suction side rim cases are lower than the full side rim cases, and this implies that the amount of the

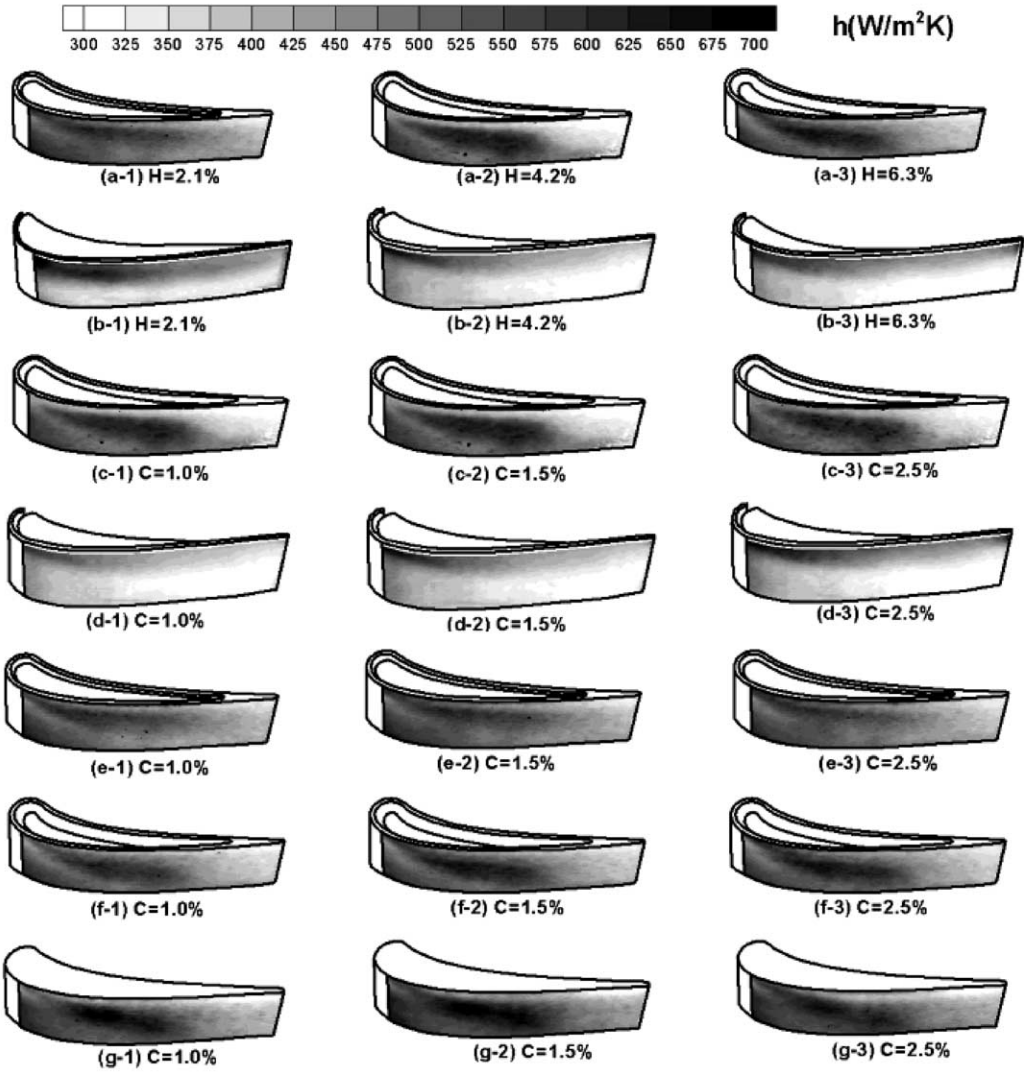

Fig. 10. Heat transfer coefficient on the near tip region of the suction side. (a) Full side rim (C = 1.5%); (b) suction side rim (C = 1.5%); (c) full side rim (H = 4.2%, [20]); (d) suction side rim (H = 4.2%, [24]); (e) full side rim (H = 2.1%); (f) full side rim (H = 6.3%); (g) plane tip [19].

leakage flow for the suction side rim cases are smaller than the full side rim cases. The reduced leakage flow for the suction side rim case results in a weaker leakage vortex, therefore, the trace of the leakage vortex is smaller than the other cases.

As the tip gap clearance increases from C = 1.0% to C = 2.5%, the heat transfer coefficient on the near tip region of the blade suction side increases for all the cases (Fig. 10(c)–(g)).

4.5. Averaged heat transfer coefficient

Fig. 11 presents the averaged heat transfer coefficient on the tip and rim surfaces. The averaged data on the shroud and near tip region of pressure and suction side were not shown because the results were not much affected by the experimental conditions compared to the tip or rim surface cases. The local heat transfer coefficients are averaged at the given X/C_x location.

On the tip surface (Fig. 11(a-1), (b-1), and (c-1)), the averaged heat transfer coefficient for the rimmed tip cases is lower than plane tip case. For the full side rim cases (a-1, b-1), the averaged heat transfer coefficient decreases as X/C_x increases due to the low heat transfer coefficient on the cavity near the trailing edge. In the mean time, the averaged heat transfer coefficient increases as X/C_x increases for the suction side rim cases (c-1). In general, the averaged heat transfer

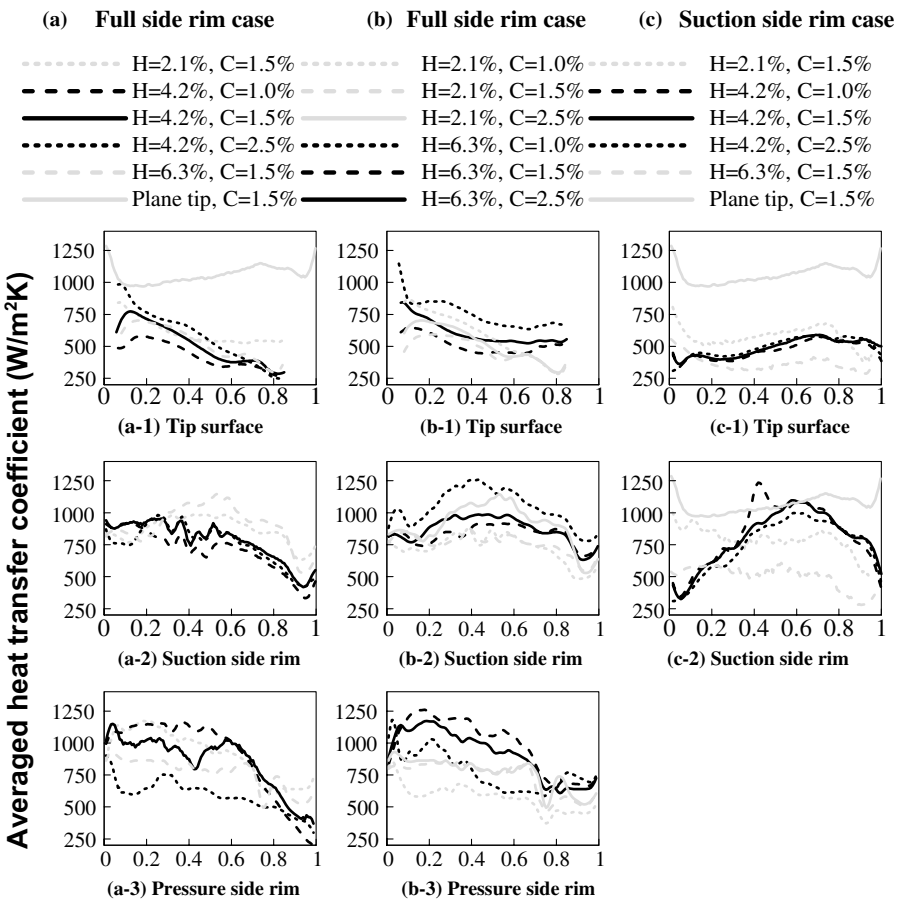

Fig. 11. Averaged heat transfer coefficient on the tip and rim surfaces.

coefficient on the tip surface generally increases as the tip gap clearance increases and rim height decreases. The effect of tip gap clearance was dominant in the full side rim cases while the suction side rim cases were more affected by the rim height. The averaged heat transfer coefficient on the rim is generally higher than that on the tip surface and was comparable to the value on the plane tip surface.

5. Conclusions

The major findings based on the experimental results are as follows:

1. By using a rimmed tip blade, the heat transfer coefficients on the blade tip and shroud were reduced significantly. However, the reduction on the blade pressure side was not remarkable.
2. The location of the high heat transfer region varied by changing the rim location, rim height and tip gap clearance.
3. As the rim height increased, the heat transfer coefficient on the tip decreased. The overall heat transfer coefficient on the tip increased as the tip gap clearance increased.
4. As the tip gap clearance increased, the overall heat transfer coefficient on the shroud increased slightly, while decreasing rim height slightly reduced the shroud heat transfer coefficient.
5. On the pressure side, the effects of the rim height, rim location, and tip gap clearance on the heat transfer coefficient were not significant.
6. On the suction side, in the suction side rim case, the heat transfer coefficient decreased as the rim height increased and as the tip gap clearance decreased. However, the effect of the rim height or tip gap clearance was not significant in the full side rim cases.
7. The overall heat transfer coefficients on the tip and near tip regions of the blade tip for the suction side rim cases are lower than that of the full side rim cases.

The observations and conclusions from this study are limited to stationary blades. Cautions should be

exercised in extending the results to rotating blades, especially on the shroud cases. In addition, the overall pressure ratio in this study was lower than in real engine conditions.

Acknowledgment

This work was prepared with the support of the NASA Glenn Research Center under grant number NAG3-2002. The NASA technical team is Mr. Robert Boyle and Dr. Raymond Gaugler. Their support is greatly appreciated.

References

[1] R.E. Mayle, D.E. Metzger, Heat transfer at the tip of an unshrouded turbine blade, in: Proc. Seventh Int. Heat Transfer Conf., Hemisphere Pub, 1982, pp. 87–92.
[2] D.E. Metzger, K. Rued, The influence of turbine clearance gap leakage on passage velocity and heat transfer near blade tips. Part I: sink flow effects on blade pressure side, ASME J. Turbomach. 111 (1989) 284–292.
[3] K. Rued, D.E. Metzger, The influence of turbine clearance gap leakage on passage velocity and heat transfer near blade tips. Part II: source flow effects on blade pressure side, ASME J. Turbomach. 111 (1989) 293–300.
[4] D.E. Metzger, R.S. Bunker, M.K. Chyu, Cavity heat transfer on a transverse grooved wall in a narrow flow channel, J. Heat Transfer 111 (1989) 73–79.
[5] M.K. Chyu, H.K. Moon, D.E. Metzger, Heat transfer in the tip region of grooved turbine blades, J. Turbomach. 111 (1989) 131–138.
[6] F.J.G. Heyes, H.P. Hodson, G.M. Dailey, The effect of blade tip geometry on the tip leakage flow in axial turbine cascades, ASME paper 91-GT-135, 1991.
[7] D.E. Metzger, M.G. Dunn, C. Hah, Turbine tip and shroud heat transfer, J. Turbomach. 113 (1991) 502–507.
[8] Y.W. Kim, J.P. Downs, F.O. Soechting, W. Abdel-Messeh, G.D. Steuber, S. Tanrikut, A summart of the cooled turbine blade tip heat transfer and film effectiveness investigations performed by Dr. D. E. Metzger, J. Turbomach. 117 (1995) 1–11.
[9] Y.W. Kim, D.E. Metzger, Heat transfer and effectiveness on film cooled turbine blade tip model, J. Turbomach. 117 (1995) 12–21.
[10] T.T. Yang, T.E. Diller, Heat transfer and flow for a grooved turbine blade tip in a transonic cascade, ASME-95-WA/HT-29, 1995.
[11] M.G. Dunn, C.W. Haldeman, Time-averaged heat flux for a recessed tip, lip, and platform of a transonic turbine blade, J. Turbomach. 122 (2000) 692–697.
[12] R.S. Bunker, J.C. Baily, A.A. Ameri, Heat transfer and flow on the first stage blade tip of a power generation gas turbine. Part 1: experimental results, J. Turbomach. 122 (2000) 263–271.
[13] G.S. Azad, J.C. Han, S. Teng, R. Boyle, Heat transfer and pressure distributions on a gas turbine blade tip, J. Turbomach. 122 (2000) 717–724.
[14] G.S. Azad, J.C. Han, R. Boyle, Heat transfer and pressure distributions on the squealer tip of a gas turbine blade, J. Turbomach. 122 (2000) 725–732.
[15] S. Teng, J.C. Han, G.S. Azad, Derailed heat transfer coefficient distributions on a large-scale gas turbine blade tip, J. Heat Transfer 123 (2001) 803–809.
[16] R.S. Bunker, J.C. Bailey, Effect of squealer cavity depth and oxidation on turbine blade tip heat transfer, ASME Paper 2001-GT-0155, 2001.
[17] G.S. Azad, J.C. Han, R.S. Bunker, C.P. Lee, Effect of squealer geometry arrangement on a gas turbine blade tip heat transfer, J. Heat Transfer 124 (2002) 452–459.
[18] D.H. Rhee, J.H. Choi, H.H. Cho, Effect of blade tip clearance on turbine shroud heat/mass transfer, ASME Paper 2001-GT-0158, 2001.
[19] J.S. Kwak, J.C. Han, Heat transfer coefficient on a gas turbine blade tip and near tip regions, Presented at the 8th AIAA/ASME Joint Thermophysics and Heat Transfer Conference, St. Louis, AIAA-2002-3012, June, 2002.
[20] J.S. Kwak, J.C. Han, Heat transfer coefficient on the squealer tip and near squealer tip regions of a gas turbine blade, Presented at the 2002 ASME International Mechanical Engineering Congress and Exposition, New Orleans, IMECE 2002-31109, November 2002.
[21] M. Papa, R.J. Goldstein, F. Gori, Effects of tip geometry and tip clearance on the mass/heat transfer from a large-scale gas turbine blade, ASME Paper GT-2002-30192, 2002.
[22] P. Jin, R.J. Goldstein, Local mass/heat transfer on a turbine blade tip, The 9th International Symposium on Transport Phenomena and Dynamics of Rotating Machinery, Honolulu, February 2002.
[23] P. Jin, R.J. Goldstein, Local mass/heat transfer on turbine blade near-tip surfaces, ASME Paper GT-2002-30556, 2002.
[24] J.S. Kwak, J. Ahn, J.C. Han, C.P. Lee, R.S. Bunker, R. Boyle, R. Gaugler, Heat transfer coefficients on the squealer tip and near tip regions of a gas turbine blade with single or double squealer, ASME Paper GT-2003-38907, 2003.
[25] A.A. Ameri and E. Steinthorsson, Prediction of Unshrouded Rotor Blade Tip Heat Transfer, ASME 95-GT-142, 1995.
[26] A.A. Ameri, E. Steinthorsson, Analysis of gas turbine rotor blade tip and shroud heat transfer, ASME 96-GT-189, 1996.
[27] A.A. Ameri, E. Steinthorsson, D.L. Rigby, Effects of tip clearance and casing recess on heat transfer and stage efficiency in axial turbines, J. Turbomach. 121 (1999) 683–693.
[28] A.A. Ameri, R.S. Bunker, Heat transfer and flow on the first stage blade tip of a power generation gas turbine. Part 2: simulation results, J. Turbomach. 122 (2000) 272–277.
[29] A.A. Ameri, D.L. Rigby, A numerical analysis of heat transfer and effectiveness on film cooled turbine blade tip models, NASA/CR 1999-209165, 1999.
[30] A.A. Ameri, Heat transfer and flow on the blade tip of a gas turbine equipped with a mean-camberline strip, J. Turbomach. 123 (2001) 704–708.

[31] A.A. Ameri, E. Steinthorsson, L.D. Rigby, Effect of squealer tip on rotor heat transfer and efficiency, ASME 97-GT-128, 1997.
[32] H. Yang, S. Acharya, S.V. Ekkad, C. Prakash, R. Bunker, Flow and heat transfer predictions for a flat-tip turbine blade, ASME paper GT-2002-30190, 2002.
[33] H. Yang, S. Acharya, S.V. Ekkad, C. Prakash, R. Bunker, Numerical simulation of flow and heat transfer past a turbine blade with a squealer-tip, ASME paper GT-2002-30193, 2002.
[34] S.J. Kline, F.A. McClintock, Describing uncertainties in single sample experiments, Mech. Eng. 75 (1953) 3–8.